Molecular Psychiatry (2008) 13, 953–969

www.nature.com/mp

ORIGINAL ARTICLE

Amyloid precursor protein and amyloid β-peptide bind to ATP synthase and regulate its activity at the surface of neural cells

C Schmidt[1], E Lepsverdize[1,5], SL Chi[2,5], AM Das[3], SV Pizzo[2], A Dityatev[1] and M Schachner[1,4]

[1]*Zentrum für Molekulare Neurobiologie, Universität Hamburg, Hamburg, Germany;* [2]*Department of Pathology, Duke University Medical Center, Durham, NC, USA;* [3]*Medizinische Hochschule Hannover, Hannover, Germany and* [4]*Keck Center for Collaborative Neuroscience and Department of Cell Biology and Neuroscience, Rutgers University, Piscataway, NJ, USA*

Amyloid precursor protein (APP) and amyloid β-peptide (Aβ) have been implicated in a variety of physiological and pathological processes underlying nervous system functions. APP shares many features with adhesion molecules in that it is involved in neurite outgrowth, neuronal survival and synaptic plasticity. It is, thus, of interest to identify binding partners of APP that influence its functions. Using biochemical cross-linking techniques we have identified ATP synthase subunit α as a binding partner of the extracellular domain of APP and Aβ. APP and ATP synthase colocalize at the cell surface of cultured hippocampal neurons and astrocytes. ATP synthase subunit α reaches the cell surface via the secretory pathway and is N-glycosylated during this process. Transfection of APP-deficient neuroblastoma cells with APP results in increased surface localization of ATP synthase subunit α. The extracellular domain of APP and Aβ partially inhibit the extracellular generation of ATP by the ATP synthase complex. Interestingly, the binding sequence of APP and Aβ is similar in structure to the ATP synthase–binding sequence of the inhibitor of F1 (IF_1), a naturally occurring inhibitor of the ATP synthase complex in mitochondria. In hippocampal slices, Aβ and IF_1 similarly impair both short- and long-term potentiation via a mechanism that could be suppressed by blockade of GABAergic transmission. These observations indicate that APP and Aβ regulate extracellular ATP levels in the brain, thus suggesting a novel mechanism in Aβ-mediated Alzheimer's disease pathology.
Molecular Psychiatry (2008) **13,** 953–969; doi:10.1038/sj.mp.4002077; published online 28 August 2007

Keywords: Alzheimer's disease; amyloid precursor protein; Aβ; ATP synthase subunit α; ATP production

Introduction

Increasing evidence suggests that amyloid precursor protein (APP) is an adhesion molecule that regulates neuronal survival, neurite outgrowth and synaptic plasticity.[1] APP is transported along axons to presynaptic terminals where it accumulates, a process that can result in amyloid β-peptide (Aβ) deposition at synapses.[2] APP is also expressed by glial cells,[3] which are important contributors to neuronal homeostasis and dynamics.[4] As a transmembrane cell surface glycoprotein, APP is a receptor that may transduce signals within the cell in response to an extracellular ligand.[5] For example, following the action of the γ-secretase that cleaves APP in the plane of the membrane, the intracellular domain of APP reaches the cell nucleus to modulate gene expression regulating apoptosis. However, neither a ligand nor downstream signaling cascades for APP has been clearly established. Nevertheless, the importance of APP in signal transduction has been documented by its ability to modulate potassium channel activity and to activate the transcription factor NF-κB.[6,7] Release of the extracellular domain of APP from presynaptic terminals has been observed in response to electrical activity.[8] This domain, in turn, regulates neuronal excitability[1] and enhances proliferation of progenitor cells in the subventricular zone.[9]

Not only is the intracellular domain of APP of functional importance, but the proteolytic fragments derived from the extracellular domain are also of interest. APP is cleaved by secretases, resulting in several fragments, including the Aβ-peptide in Alzheimer's disease.[10] An increase in the generation of Aβ is, according to the amyloid hypothesis of Alzheimer's disease, the trigger for disease pathogenesis.[11] Aβ has been implicated in multiple functions, particularly in cytotoxicity of its oligomeric forms,[12,13] although their functional roles are not fully understood. Synapses

Correspondence: Professor M Schachner, Zentrum für Molekulare Neurobiologie, Universität Hamburg, Martinistr 52, Hamburg 20246, Germany.
E-mail: melitta.schachner@zmnh.uni-hamburg.de
[5]These authors contributed equally to this work.
Received 12 November 2006; revised 22 February 2007; accepted 12 April 2007; published online 28 August 2007

may be particularly susceptible to the adverse effects of Aβ as it impairs synaptic ion and glucose transporters and damages neurons by inducing oxidative stress and disrupting cellular calcium homeostasis.[14] Consistent with the notion that Aβ deposition may exert neurotoxic effects are the observations that in APP-mutant mice with enhanced Aβ production, memory deficits develop early in the process of Aβ deposition.[15] Interestingly, Aβ is not only deposited in the brain tissue itself, but also at the luminal surface of brain blood vessels where it induces pathological reactions including hemorrhage, death of endothelial cells and constriction of capillaries which are confounding factors in Alzheimer's disease.[16]

In our search for APP-binding partners, we have identified the α-subunit of F_1F_0-ATP synthase, also termed complex V, which facilitates ATP production from the transmembrane proton-motive force generated by the mitochondrial respiratory chain.[17] The F_1F_0-ATP synthase complex not only generates ATP but also hydrolyzes ATP and by this action facilitates a proton gradient.[18] Although first described as a predominantly mitochondrial protein, the entire F_1F_0-ATP synthase complex has also been localized to the cell surface of endothelial cells, fibroblasts and hepatocytes, where the complex produces ATP extracellularly.[19–22] Our observations demonstrate a novel function for APP and Aβ in regulating ATP synthase activity through interaction with the α subunit of ATP synthase. ATP is thus not only the main energy source of mammalian cells, but also an important extracellular signaling molecule with multiple functions.[23]

Materials and methods

Antibodies and animals

The following antibodies were used: 7H10 (a mouse monoclonal anti-ATP synthase subunit α; Molecular Probes, Eugene, OR, USA), D3 (a mouse monoclonal antibody against the intracellular domain of the mouse NCAM 180 isoform of the neural cell adhesion molecule[24]), C-20 (anti-synaptophysin antibody; Santa Cruz Biotechnology, Santa Cruz, CA, USA), 22723 (rabbit polyclonal antibodies, directed against the extracellular domain of mouse APP), 22C11 (a mouse monoclonal antibody directed against the amino acid sequence 60–100 of human APP) and WO-2 (a monoclonal mouse antibody directed against amino acids 1–16 of human Aβ). The monoclonal antibodies against APP and Aβ were kind gifts from G Multhaup (Free University of Berlin, Berlin, Germany). Synthetic human Aβ1–40 was purchased from Schafer-N (Copenhagen, Denmark). C57BL/6J mice were used for all studies. The APP 23 transgenic mouse strain (a kind gift from M Staufenbiel, Hoffmann-La Roche, Basel, Switzerland) overexpressing the Swedish mutation of human APP under the control of the Thy-1 promoter[25] was used in parallel with the respective wild-type controls derived from the same breeding colony.

Preparation of APP-Fc and APP-α-Fc

Mouse APP 695 cDNA encoding for the neuronal isoform of APP (a kind gift from S Sisodia, University of Chicago, Chicago, IL, USA) was subcloned into the pblue Bac vector using the *Bam*HI and *Sac*I restriction sites. To generate the fusion protein containing the extracellular domain of APP with the Fc part of human immunoglobulin G (IgG) at its C-terminal end (APP-Fc), primers for the *Sac*I restriction site at the 5′end (CTGACGGAACCAAGACCACCG) and for the C-terminal end of the APP extracellular domain (terminating at amino acid position 624; SWISS-PROT accession number P12023) at the 3′end (GCTGAAGATGTGGGTTCGAACAAA) were used, introducing a new *Bcl*I restriction site at the 3′end. To generate APP-α-Fc, the primer of the 5′end *Sac*I restriction site and the 3′end the α-secretase cleavage site (APP-α-Fc) were also used to introduce a new *Bcl*I site. Via this new *Bcl*I restriction site, the PCR products were ligated to the human Fc-tag in the pIG(+) vector and subsequently the *Bam*HI/*Sac*I restriction product of the mouse APP 695 was ligated using the *Sac*I restriction site. The whole construct was cut out using the *Hind*III and *Xba*I restriction site of the pIG(+) and ligated into the pcDNA 3(+) vector. This vector was used to stably transfect Chinese hamster ovary K1 cells according to published procedures.[26] CHL1-Fc and PrP-Fc that contain the extracellular domain of these adhesion molecules in fusion with Fc were expressed and, as for the APP-Fc fusion proteins, purified via the Fc-tag using a Protein-A column chromatography as described.[26]

Cell culture

B103 cells that do not express APP[27] were stably transfected with pcDNA 3.1(−) containing the human cDNA sequence of APP 695, the predominantly neuronal expressed isoform of APP.[3] Cells were maintained in Dulbecco's modified Eagle's medium containing 10% fetal bovine serum and 5% horse serum supplemented with hygromycin for selection. Dissociated cultures of early postnatal hippocampus were prepared as described.[28] The cultures were maintained in neurobasal medium supplemented with B26 for at least 12 days before immunocytochemical staining. Cultures contained predominantly neurons, but also glial fibrillary acidic protein immunoreactive astrocytes.

Immunocytochemistry

For detection of APP both at the cell surface and intracellularly, cultures of hippocampal cells were incubated for 30 min at room temperature (RT) with 4% formaldehyde in phosphate-buffered saline (PBS), followed by incubation in PBS supplemented with 10% horse serum, 0.2% bovine serum albumin (BSA) and 0.3% Triton X-100 for permeabilization. After incubation with primary antibodies against APP (22734, diluted 1:1000) and synaptophysin (1:200) for 3 h at RT, cells were again washed with PBS. Immunostaining with secondary antibody was carried

out with antibodies against rabbit IgG (anti-rabbit 488, Alexa; Molecular Probes) and goat IgG (anti-goat 488, Jackson ImmunoResearch, Cambridgeshire, UK). After washing with PBS, cells were mounted with Aqua Polymount (Polyscience Inc., Washington, PA, USA). Samples were examined with a laser scanning confocal microscope (Leica TCS SP2).

For detection of cell surface–localized APP and ATP synthase subunit α, live cells were incubated with antibodies 7H10 (diluted 1:100) and 22734 (diluted 1:250) for 1 h at 4 °C. Cultures were then washed two times with ice-cold PBS and incubated with secondary antibodies at 4 °C as specified in the previous paragraph. Experiments were carried out at 4 °C to prevent internalization of cell surface–localized proteins.[29,30]

Colocalization experiments of ATP synthase subunit α and the synaptic marker synaptophysin were performed to analyze the synaptic distribution of cell surface ATP synthase subunit α. For this study, the protocol for cell surface detection of ATP synthase subunit α was applied, followed by the protocol for immunostaining after fixation with paraformaldehyde (see first paragraph of this subheading). Twenty-five punctate dots of ATP synthase subunit α immunostaining per visual field were analyzed for colocalization with synaptophysin immunostaining. Two cultures were used for analysis of colocalization, and for each culture three visual fields were evaluated.

Isolation of a crude mitochondrial fraction from mouse brain

Isolation of mitochondria was performed as described.[31] Briefly, mice were killed by carbon dioxide intoxication and brains were quickly removed. Brains were homogenized by 10–15 strokes in a Dounce-type glass homogenizer in homogenization buffer H1 (75 mM sucrose, 225 mM sorbitol, 1 mM ethylene glycol tetraacetic acid, 10 mM Tris-HCl (pH 7.5) and 0.1% BSA). Homogenates were centrifuged at 1000 *g* and 4 °C for 10 min. The supernatants were collected and pelleted by centrifugation at 12 000 *g* and 4 °C for 10 min. The pellets were resuspended in 10 volumes of H1 buffer and centrifuged at 14 000 *g* and 4 °C for 5 min. This step was repeated seven times. The pellet from the last centrifugation step was resuspended in three volumes of H1 buffer and frozen at −80 °C for further use.

Purification of mammalian F_1F_0-ATP synthase complex from murine heart tissue

Mice were killed by carbon dioxide intoxication and hearts were quickly removed. To obtain fresh murine heart mitochondria the heart tissue was treated as described above for isolation of a crude mitochondrial fraction. Mitochondria were washed three times with 250 mM sucrose solution supplemented with 2 mM EDTA (pH 8.8) to remove possible contamination with BSA. Preparation of submitochondrial particles and purification of the F_1F_0-ATP synthase complex were accomplished as previously described.[31]

Preparation of a synaptosomal fraction

Mice were exposed to carbon dioxide intoxication and the brains were immediately removed and homogenized by 10–15 Potter strokes in Homo-buffer (50 mM Tris-HCl (pH 7.5), 0.32 M sucrose, 1 mM $CaCl_2$ and 1 mM $MgCl_2$) on ice. The homogenate was centrifuged at 1000 *g* and 4 °C for 10 min and the supernatant was subjected to a 17 000 *g* centrifugation step at 4 °C for 15 min. The resulting pellet was resuspended in Homo-buffer and laid on top of a sucrose gradient consisting of two steps of 1.2 and 1.0 M sucrose solution in 50 mM Tris-HCl (pH 7.5), 1 mM $CaCl_2$ and 1 mM $MgCl_2$. The synaptosome-enriched fraction was collected by centrifugation at 100 000 *g* and 4 °C for 2 h. The fraction at the interface between the 1.2 and 1.0 M sucrose interface was collected and pelleted by a 100 000 *g* centrifugation step at 4 °C for 1 h. The pellet was resuspended in PBS and stored at −80 °C for further use.

Biochemical cross-linking with sulfo-SBED

All steps for biochemical cross-linking were performed under light protection. APP-Fc or CHL1-Fc (100 μg each) was incubated in 500 μl PBS with 10 μl of sulfo-SBED (sulfosuccinimidyl-2-[6-(biotinamido)-2(*p*-azidobenz-amido) hexa-noamido]ethyl-1,3′-dithiopropionate; Perbio, Rockford, IL, USA) dissolved at 1 mg per 25 μl dimethyl sulfoxide for 30 min at RT. The sample was then dialyzed using a Slide-a-lyzer mini dialysis unit (Perbio) and added afterwards to 50 μl solution of Protein-A magnetic beads (Dynal, Hamburg, Germany). The mixture was incubated for 1 h at RT. The magnetic beads were washed six times with PBS using a magnet. Beads containing the bait in the form of Fc fusion proteins were then incubated overnight at 4 °C with subfractions of brain homogenates prepared from 10 brains of 2- to 3-month-old C57BL/6 mice. The samples were transferred to a 40 × 10 cm cell culture dish, placed on ice and exposed to UV light for 15 min using an ultraviolet cross-linker (Amersham, Buckinghamshire, UK) at an energy setting of 365. Beads were washed two times with PBS, two times with PBS containing 0.5% Triton X-100 and two times with PBS containing 1% Triton X-100. Bound bait/prey proteins complexes were removed from the beads by 10 min incubation with elution buffer (0.1 M glycine (pH 2.3) and 0.5 M NaCl). After magnetic removal of the beads, the solution containing the bait/prey complex was neutralized with 5 μl of neutralization buffer (1.5 M Tris-HCl, pH 8.0) and subsequently boiled in sodium dodecyl sulfate (SDS) sample buffer containing dithiothreitol to separate bait from prey. Biotinylated prey proteins were separated by SDS-polyacrylamide gel electrophoresis (PAGE) and probed with horseradish peroxidase (HRP)–coupled streptavidin.[32]

For identification of the binding partners, which are the prey of the APP-Fc bait, 5–10% SDS-PAGE gels were silver stained[33] and silver-stained bands were subjected to nanoelectrospray mass spectrometry in a QTOF II instrument (Micromass, Manchester, UK), kindly performed by Fritz Buck (Institut für Zellbiochemie und Klinische Neurobiologie, University Medical Center Hamburg-Eppendorf, Germany).

Pull-down assay

The pull-down assay was performed to identify binding partners using Fc-fusion proteins coupled to beads as bait. For preclearing, the Protein-A magnetic beads (50 µl, Dynal) were added to crude brain mitochondrial fraction diluted 1:4 in buffer A (50 mM Tris-HCl (pH 7.5), 1 mM $CaCl_2$, 1 mM $MgCl_2$ and 0.1% Triton X-100) supplemented with protease inhibitor cocktail (Roche, Mannheim, Germany). The mixture was allowed to react for 1 h at 4 °C. Beads were then removed using a magnet. For binding of the bait to the Protein-A magnetic beads, 50–100 µg of Fc-tagged bait protein were incubated for 30 min at RT with 100–200 µl of Protein-A magnetic beads in buffer B (50 mM Tris-HCl (pH 7.5), 1 mM $CaCl_2$ and 1 mM $MgCl_2$). The bait/Protein-A complex was washed four times with buffer B using a magnet and added to the precleared crude fraction of brain mitochondria. After 35 min incubation on a tumbling wheel at RT, the samples were washed three times with buffer B and three times with buffer A. The bait/prey complex was eluted by 10 min incubation with elution buffer (0.1 M glycine (pH 2.3) and 0.5 M NaCl). After removing the beads the samples were neutralized with 5 µl of neutralization buffer (1.5 M Tris-HCl, pH 8.0). The samples were boiled in SDS sample buffer, separated by SDS-PAGE and subjected to western blot analysis.

The pull-down assay was also performed using Aβ as bait. A total of 10 µg WO-2 or D3 antibodies were added to 150 µl Protein-G magnetic beads (Dynal) and incubated in PBS for 1 h at RT. The antibody/Protein-G complex was cross-linked with the chemical cross-linker BS^3 (Perbio) in 500 µl PBS (1 mg BS^3 ml^{-1}) by incubation for 1 h at RT. Preclearing of the mitochondrial fraction and washing steps were performed as described in the previous paragraph. To saturate the mitochondrial ATP synthase subunit α with Aβ, 100 µg Aβ per sample was added to the crude mitochondrial fraction after preclearing. After the last washing step, beads were boiled in SDS sample buffer and removed by a short centrifugation step. Supernatants were subjected to SDS-PAGE and western blot analysis.

Cell surface biotinylation

B103 cells were grown to near confluence in a 10 cm culture dish. For the experiment they were placed on ice and washed twice with ice-cold PBS-CM (PBS containing 0.5 mM $CaCl_2$, 2 mM $MgCl_2$). For surface biotinylation the cells were incubated 10 min on ice with PBS-CM supplemented with 0.5 mg ml^{-1} Sulfo-NHS-LS-biotin (Perbio). The solution was then removed from the cells and the biotinylation reaction was terminated by incubation with PBS-CM supplemented with 20 mM glycine for 5 min. After two washes with ice-cold PBS-CM, cells were lysed by a 30 min incubation at 4 °C with radioimmunoprecipitation assay (RIPA) buffer (50 mM Tris-HCl (pH 7.4), 150 mM NaCl, 1 mM EDTA and 1% NP40) supplemented with protease inhibitor cocktail (Roche). To remove nuclei, the lysates were centrifuged at 1000 *g* and 4 °C for 5 min. Streptavidin magnetic beads (150 µl, Dynal) were added to the supernatants and the samples were incubated overnight on a tumbling wheel at 4 °C. The streptavidin-coupled beads were then washed four times with RIPA buffer using a magnet, and boiled in SDS sample buffer. Beads were then removed by centrifugation. The supernatants were boiled in sample buffer, separated by SDS-PAGE and subjected to western blot analysis.

To prepare cell lysate, 3×10^6 B103 wild-type cells were lysed through two freeze and thaw cycles. To remove crude cell debris the lysate was centrifuged at 700 *g* for 5 min at 4 °C. The supernatants were added 4 h prior to experiment to the dishes.

For the examination of the cell surface transport, brefeldin A (Merck, Darmstadt, Germany) was used. Brefeldin A (5 µM) was supplemented to the cell culture media 4 h before the experiment and cell surface biotinylation was then carried out as described above.

For analysis of N-glycosylation of ATP synthase subunit α, biotin-labeled cell surface proteins were purified by streptavidin beads. Beads were then washed three times with PBS and 0.5% Triton X-100 using a magnet and incubated with 2U PNGase F (Roche) in 500 µl PBS and 0.5% Triton X-100 for 18 h at 37 °C. After three washing steps with PBS by use of a magnet, the samples were boiled in SDS sample buffer and the beads were removed by centrifugation. The supernatants were used for western blot analysis.

Enzyme-linked immunosorbent assay

Enzyme-linked immunosorbent assay (ELISA)–based binding tests were performed as described[34] with 10 µg ml^{-1} APP-Fc or human Aβ (1–40) used for substrate coating. Coating was performed in PBS supplemented with 1 mM $CaCl_2$ and 1 mM $MgCl_2$ (PBS-CM) overnight at 4 °C. Washing steps were performed in PBS-CM with 0.05% Tween 20. For competition assays, soluble F_1-ATP synthase complex was pre-incubated for 1 h at 37 °C in the presence or absence of a five times molar excess of recombinantly produced IF_1, and then introduced to the coated wells. Monoclonal anti-ATP synthase subunit α (7H10; 0.5 µg ml^{-1}) and HRP-coupled secondary antibodies (Perbio, Rockford) in PBS-CM containing 1% BSA were used for detection. A total of 100 µl of freshly prepared staining solution, 0.5 mg ml^{-1} *o*-phenylenediamine dihydrochloride in stable peroxide substrate buffer (Perbio), was added and the reaction was stopped after 15 min by addition of 2.5 M

H_2SO_4. Bound conjugates were quantified by measuring absorbance at 490 nm.

ATP generation by bioluminescent luciferase assay
These studies were performed as described previously.[35]

Purification of His-tagged ATP synthase subunit α and His-tagged IF_1
Competent *Escherichia coli* BL21DE3 were transformed with the pET-24a His-ATP synthase subunit α vector or pET 15b human IF_1. His-tagged ATP synthase subunit α was expressed in *E. coli*,[35] and His-tagged-IF_1.[36] The His-tagged ATP synthase subunit α and the IF_1 were batch purified using Qiagen Ni-NTA-agarose under native conditions according to the manufacturer's instructions.

Co-immunoprecipitation
Co-immunoprecipitations were performed in crude brain mitochondrial fractions from either wild-type or APP23 transgenic mice. A total of 150 µl of Protein-G magnetic beads (Dynal) were incubated with 10 µg of WO-2 antibody for 1 h at RT in 500 µl PBS. To couple the antibody to the beads, 500 µl PBS plus the cross-linker BS^3 (1 mg ml^{-1}; Perbio) were incubated for 1 h at RT. To remove unbound cross-linker the beads were washed with buffer B (50 mM Tris-HCl (pH 7.5), 1 mM $CaCl_2$ and 1 mM $MgCl_2$) for four times using a magnet. Crude brain mitochondrial fractions were diluted in buffer A (50 mM Tris-HCl (pH 7.5), 1 mM $CaCl_2$, 1 mM $MgCl_2$ and 0.1% Triton X-100) plus protease inhibitor mix (Roche) 1:5 and then precleared by incubation with 50 µl Protein-G magnetic beads for 3 h at 4 °C on a rotating wheel. Antibody/Protein-G complex was mixed with the precleared crude brain mitochondrial fraction and incubated overnight at 4 °C on a rotating wheel. Samples were washed four times with buffer B and four times with buffer A using a magnet. After the washing steps, 50 µl SDS sample buffer was added to the beads and the probe was subsequently boiled. The beads were removed by a short centrifugation step and the supernatants were used for western blot analysis.

Western blot analysis
Before western blot analysis, total protein content of the samples was determined by BCA test (Perbio) according to the manufacturer's instructions. The samples were separated by SDS-PAGE and transferred to nitrocellulose membranes (Schleicher & Schuell, Dassel, Germany) by tank blotting. The membranes were incubated with primary antibody overnight at 4 °C. For detection of ATP synthase subunit α, the mouse monoclonal antibody 7H10 (0.5 µg ml^{-1}) was used. The signals were revealed using HRP-conjugated secondary antibodies (1:10 000) followed by ECL detection (Supersignal, Perbio).

Quantification of secreted and cellular APP
For determination of secreted APP levels, conditioned medium from the hippocampal cell cultures was centrifuged at 700 *g* for 5 min at RT. The supernatant was mixed with SDS sample buffer and boiled for 5 min. Quantification of APP content in hippocampal cells was done by 30 min cell lysis in RIPA buffer supplemented with protease inhibitor mix (Roche) at 4 °C, centrifugation of samples for 5 min at 1000 *g* and 4 °C and western blot analysis with the primary antibody 22C11 (1:10 000) to detect APP.

Measurement of F_1F_0-ATP synthase complex ATPase activity
The ATPase activity of F_1F_0-ATP synthase was measured as described previously.[37]

Electrophysiological recordings
Two- to three-month-old C57Bl/6J mice of both sexes were used for the electrophysiological experiments. Hippocampal slice preparation and recordings of long-term potentiation (LTP) at CA3-CA1 synapses were performed as described elsewhere.[38,39] Briefly, after CO_2 anesthesia, decapitation and removal of the brain, the hippocampi were cut with a vibratome in 350 µm thick slices in ice-cold artificial cerebrospinal fluid (ACSF) containing: 250 mM sucrose, 25 mM $NaHCO_3$, 25 mM glucose, 2.5 mM KCl, 1.25 mM NaH_2PO_4, 2 mM $CaCl_2$ and 1.5 mM $MgCl_2$ (pH 7.3). The slices were then kept at RT in a chamber filled with carbogen-bubbled ACSF, containing 125 mM NaCl instead of 250 mM sucrose, for at least 2 h before the start of recordings. In the recording chamber, slices were continuously superfused with carbogen-bubbled ACSF (3 ml min^{-1}) at RT.

Stimulation of Schaffer collateral/commissural fibers and recordings of focal field excitatory postsynaptic potential (fEPSP) were performed in the *stratum radiatum* with glass pipettes filled with ACSF and having a resistance of 1–2 MΩ. Basal synaptic transmission was monitored at 0.05 Hz. The inter-theta burst stimulation (TBS) interval was 20 s and five TBSs were applied to induce LTP. TBS consisted of 10 bursts. Bursts were delivered at 5 Hz. Each burst consisted of four pulses delivered at 100 Hz. In one series of experiments, the number of stimulation pulses was reduced two times by reducing the number of bursts from ten to five, as indicated in 'Results'. Duration of pulses was 0.2 ms and stimulation strength was set such as to provide baseline fEPSPs with amplitudes of approximately 50% from the subthreshold maximum. Aβ was prepared in 2.5 µM stock solution prior to experiment, incubated 16 h at RT to enhance oligomerization and shock frozen after this time in liquid nitrogen. The stock solution was thawed immediately before experiment and used after appropriate dilution. ACSF containing 500 nM Aβ or 300 nM IF_1 was applied to slices 20–30 min before induction of LTP to provide sufficient time for penetration of these compounds.[40] Picrotoxin, an inhibitor of $GABA_A$ receptors, was applied alone or together with Aβ (Schafer-N) or IF_1 at a concentration of 100 µM. Statistical comparison of the levels of short-term potentiation (STP) and LTP

under different experimental conditions was performed using the two-tailed *t*-test or one-way analysis of variance. *P*-values smaller than 0.05 were accepted as providing significant differences between compared groups.

Results

APP and Aβ interact with ATP synthase subunit α

To search for ligands of the extracellular domain of APP, we fused the whole extracellular domain of mouse APP with human Fc (APP-Fc) and labeled the fusion protein with the trifunctional cross-linker sulfo-SBED via primary amines of APP. Sulfo-SBED transfers its biotin group after a short incubation with UV light to the binding partners (prey) of the fusion protein (bait) that was immobilized via its Fc portion on Protein-A-coupled magnetic beads. After cross-linking, the bait/prey complex was separated from the beads by dissociating the Protein-A/Fc complex. The eluted proteins were then boiled in SDS sample buffer containing dithiotreithol to separate the biotinylated prey proteins from the non-biotinylated baits. Incubation of APP-Fc with a synaptosome-enriched fraction of mouse brain resulted in bound ATP synthase subunit α as biotinylated protein, and therefore as a possible interaction partner of APP (Figure 1a, lane 2). When CHL1-Fc comprising the extracellular domain of the close homolog of L1 in fusion with Fc was used as a bait control, the band corresponding to ATP synthase subunit α was not detectable (Figure 1a, lane 1). We were not able to identify other bands as putative binding partners of APP in this experiment via mass spectroscopy (Figure 1a, lane 2), with the exception of APP (arrowhead) that displayed in our experiments a homophilic binding, as previously described.[41]

To verify this interaction we performed a pull-down experiment with APP-Fc coupled to Protein-A beads as bait in a crude homogenate of mouse brain mitochondria (Figure 1b). ATP synthase subunit α was pulled down from the homogenate with APP-Fc, but not with CHL1-Fc or Fc alone (Figure 1b, lane 4, arrow). In contrast to the full-length extracellular domain, the α-secretase cleaved form of APP (APP-α-Fc) did not pull down ATP synthase subunit α (Figure 1c). To analyze if Aβ would also bind to ATP synthase subunit α, synthetic human Aβ peptide was pre-incubated with the monoclonal antibody WO-2, which binds to the first 16 amino acids of human Aβ. This antigen/antibody complex was then incubated with the crude mitochondrial homogenate and a protein was pulled down that reacted by western blot analysis with antibodies against mouse ATP synthase subunit α (Figure 1d, lane 2). A monoclonal antibody against the intracellular domain of the NCAM 180 isoform was also incubated with Aβ for control and did not co-isolate a band with the molecular weight of ATP synthase subunit α (Figure 1d, lane 1). Only the bound synthetic human Aβ peptide, and not the endogenous murine Aβ or full-length murine APP, was used as a bait in these tests, since the WO-2 antibody recognizes only human, but not murine APP.[42] Thus, not only full-length APP binds to ATP synthase subunit α, but also its proteolytic product Aβ is a ligand for the enzyme.

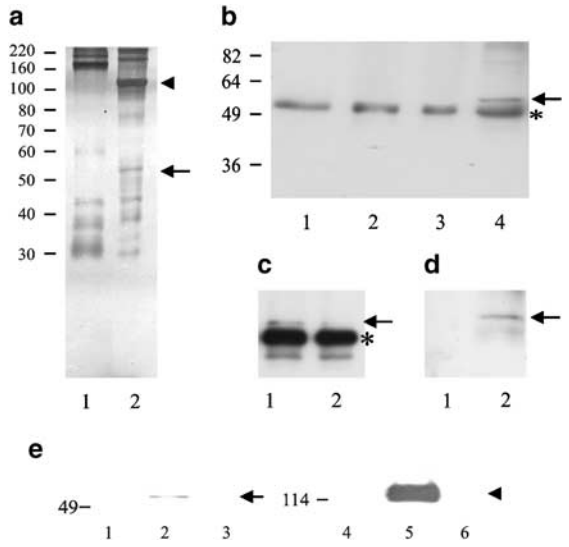

Figure 1 The extracellular domain of APP and Aβ interact with ATP synthase subunit α. (**a**) Sulfo-SBED mediated cross-linking of APP-Fc or CHL1-Fc as bait with prey proteins from a mouse synaptosomal fraction shows that ATP synthase subunit α interacts with the extracellular domain of APP. Lane 1, eluate of CHL1-Fc-coated beads (control); lane 2, eluate of APP-Fc-coated beads. The indicated bands were identified via mass spectroscopy as ATP synthase subunit α (arrow) and APP (arrowhead). (**b**) Pull-down experiments show that ATP synthase subunit α interacts with the extracellular domain of APP. Pull-down experiments were performed using 0.1% Triton X-100 detergent-solubilized crude mouse brain mitochondrial fraction. Lane 1, pull-down with Protein-A magnetic beads alone; lane 2, with CHL1-Fc; lane 3, with human Fc; lane 4, APP-Fc. Arrow, ATP synthase subunit α. The asterisk indicates nonspecific binding of the secondary antibody. (**c**) Pull-down experiments with APP-Fc and APP-α-Fc from a mouse brain mitochondrial fraction show that only APP-Fc interacts with ATP synthase subunit α. Lane 1, pull-down with APP-Fc and lane 2 with APP-α-Fc. Arrow, ATP synthase subunit α. The asterisk indicates nonspecific binding of the secondary antibody. (**d**) Aβ pulls down ATP synthase subunit α from crude brain mitochondrial fraction. Lane 1, NCAM antibody D3 pre-incubated with Aβ; lane 2, antibody WO-2 pre-incubated with Aβ. Arrow, ATP synthase subunit α. (**e**) Co-immunoprecipitation of APP and ATP synthase subunit α using detergent-solubilized crude brain mitochondrial fraction of APP23 transgenic and age-matched wild-type mice with antibody WO-2. Lane 1, Protein-G beads alone with the fraction from APP23 mice; lane 2, antibody WO-2 on Protein-G beads with the fraction from APP23 mice; lane 3, antibody WO-2 on Protein-G beads with the fraction of wild-type mice. Membranes were stripped and then probed with antibody 22C11 against APP. Lanes 4, 5 and 6 represent the stripped lanes of lanes 1, 2 and 3, respectively. Arrow, ATP synthase subunit α; arrowhead, APP.

To verify the association of APP or Aβ with ATP synthase subunit α under more physiological conditions of APP or Aβ with ATP synthase subunit α, a co-immunoprecipitation experiment was carried out (Figure 1e). The antibody WO-2 was used to immunoprecipitate APP or Aβ from detergent lysates (0.1% TritonX-100) of crude brain mitochondria homogenate isolated from transgenic mice overexpressing the human APP under the control of the Thy-1 promoter (APP23 mice). ATP synthase subunit α was detected in the WO-2 immunoprecipitate by western blot analysis (Figure 1e, lane 2). As a negative control, age-matched wild-type mice were used for the immunoprecipitation in parallel. As WO-2 does not recognize the murine form of APP or Aβ (Figure 1d, lane 6), ATP synthase subunit α was not co-immunoprecipitated (Figure 1e, lane 3).

After transfection of APP 695 in the APP-deficient B103 wild-type cell line, cell surface localization of biotin-labeled ATP synthase subunit α was significantly increased in the APP 695-transfected cells compared to that in nontransfected cells (Figure 2a–d). So cell surface APP increases the cell surface localization of endogenous ATP synthase subunit α. Our experiments were not able to dissect if this increase is due to amplification of transport to the cell membrane by APP or by action of APP as a cell surface receptor for soluble ATP synthase subunit α. It should also be noted that in the nontransfected B103 cells a faint ATP synthase subunit α immunoreactive band was observed (Figure 2a, lane 1), suggesting the existence of another binding partner at the cell surface.

ATP synthase subunit α is not a transmembrane constituent, but associates as a soluble component with the other components in the F_1F_0-ATP synthase complex of mitochondria and at the cell surface. We examined whether soluble ATP synthase subunit α could bind to APP at the cell surface under physiological conditions. This was tested by adding soluble ATP synthase subunit α to neuroblastoma B103 cells transfected to express APP at the cell surface and nontransfected parental cells as negative control. In the first experiment, we used nontransfected B103 cell lysate, highly enriched in soluble mitochondrial ATP synthase subunit α (data not shown), as a source for ATP synthase subunit α. We incubated B103 cells transfected with APP 695 and nontransfected B103 cells for 4 h with the cell lysate and performed a surface biotinylation. Only in APP-transfected cells did we observe a band of mitochondrially derived, and therefore non-glycosylated, ATP synthase subunit α (Figure 2e, lane 4). In a second experiment, we used ATP synthase subunit α recombinantly produced in bacteria and purified via N-terminal linked His-tag. When this ATP synthase subunit α construct was added to cultures of nontransfected or APP 695-transfected neuroblastoma cells, ATP synthase subunit α was detected only in the transfected cells after cell surface biotinylation and isolation by streptavidin beads (Figure 2f, lane 4). The combined data provide evidence that soluble ATP synthase subunit α binds APP under physiological conditions at the cell surface.

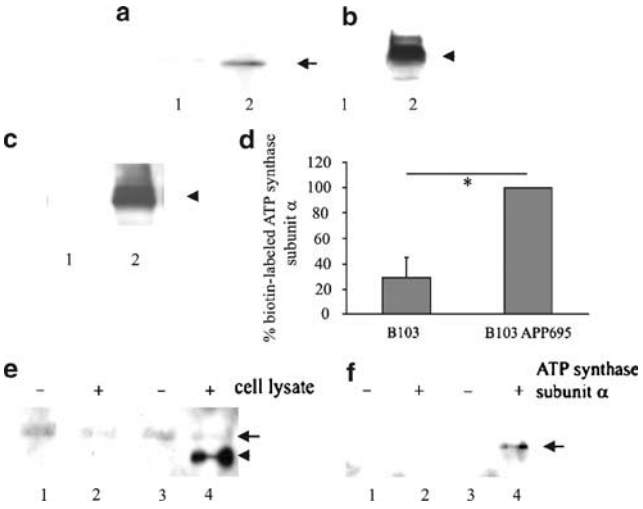

Figure 2 Cell surface expression of APP enhances the cell surface localization of ATP synthase subunit α. (**a**) Lane 1, cell surface biotinylation, precipitation with streptavidin beads and detection with 7H10 in nontransfected B103 cells; lane 2, APP 695-transfected B103 cells. (**b**) Levels of secreted APP isoforms in the stably APP transfected B103 cells. Lane 1, nontransfected B103 cells; lane 2, APP 695-transfected B103 cells. (**c**) Levels of cellular APP isoforms in stably APP transfected B103 cells. Lane 1, nontransfected B103 cells; lane 2, APP 695-transfected B103 cells. Arrow, ATP synthase subunit α; arrowheads, APP. (**d**) Diagram with quantification of immunoblots from the cell surface biotinylation experiments. For each experiment the levels of biotinylated ATP synthase subunit α in the APP 695-transfected B103 cells were set as 100%. Mean values ± s.d. ($n = 4$) are shown, Wilcoxon test with a significance of $^*P < 0.05$ between B103 and APP 695-transfected B103 cells. (**e**) Cell surface biotinylation of ATP synthase subunit α is increased in APP 695-transfected B103 cells, but not in nontransfected B103 cells, after incubation with cell lysate containing ATP synthase subunit α or with purified His-tagged ATP synthase subunit α. Lanes 1 and 2, nontransfected B103 cells; lanes 3 and 4, APP 695 transfected B103 cells, which were incubated with cell lysate. The total protein content of lanes 1 and 2 was three times higher than that in lanes 3 and 4. Arrow, glycosylated ATP synthase subunit α; arrowhead, non-glycosylated ATP synthase subunit α from the cell lysate. (**f**) Lanes 1 and 2, nontransfected B103 cells; lanes 3 and 4, APP 695-transfected B103 cells incubated with His-tagged ATP synthase subunit α. Equal amounts of protein were loaded in each lane. Arrow, ATP synthase subunit α.

In an ELISA, APP and Aβ bound directly to the F_1 part of the ATP synthase complex (Figure 3a). For this assay, we coated APP-Fc or synthetic Aβ1–40 and analyzed the binding of different concentrations of soluble F_1F_0-ATP synthase complex purified from a mitochondrial fraction of mouse heart tissue. Binding to APP-Fc and Aβ was dose dependent and saturable. There was no significant binding of the F_1F_0-ATP synthase complex to the BSA control.

As APP-Fc and Aβ both bind to the ATP synthase subunit α (Figures 1b and d), it is likely that APP binds to the enzyme via the extracellular sequence shared between APP and Aβ. Thus, Aβ should compete with APP for binding to the ATP synthase subunit α. Therefore, we performed a pull-down experiment using APP-Fc as bait with a detergent-solubilized homogenate from a crude brain mitochondrial fraction. Pre-incubation with a 10-fold excess of Aβ, but not a control peptide derived from the extracellular part of APP (amino acids 395–410; SWISS-PROT accession number P05067) reduced the amount of ATP synthase subunit α pulled down by APP-Fc (Figure 3b).

A different assay was used to show that APP-dependent binding of ATP synthase subunit α to the cell surface is influenced by Aβ. In this assay, binding of ATP synthase subunit α was measured after cells that constitutively express and secrete the enzyme were pre-incubated with Aβ. Then, cell surface biotinylation was performed to determine if the enzyme had attached to the cell surface. Pre-incubation of B103 neuroblastoma cells with Aβ reduced the cell surface attachment of ATP synthase subunit α when applied to B103 cells transfected with APP 695 (Figure 3c, compare lanes 1 and 2). We next determined if the binding of mitochondria-derived, non-glycosylated ATP synthase subunit α was also

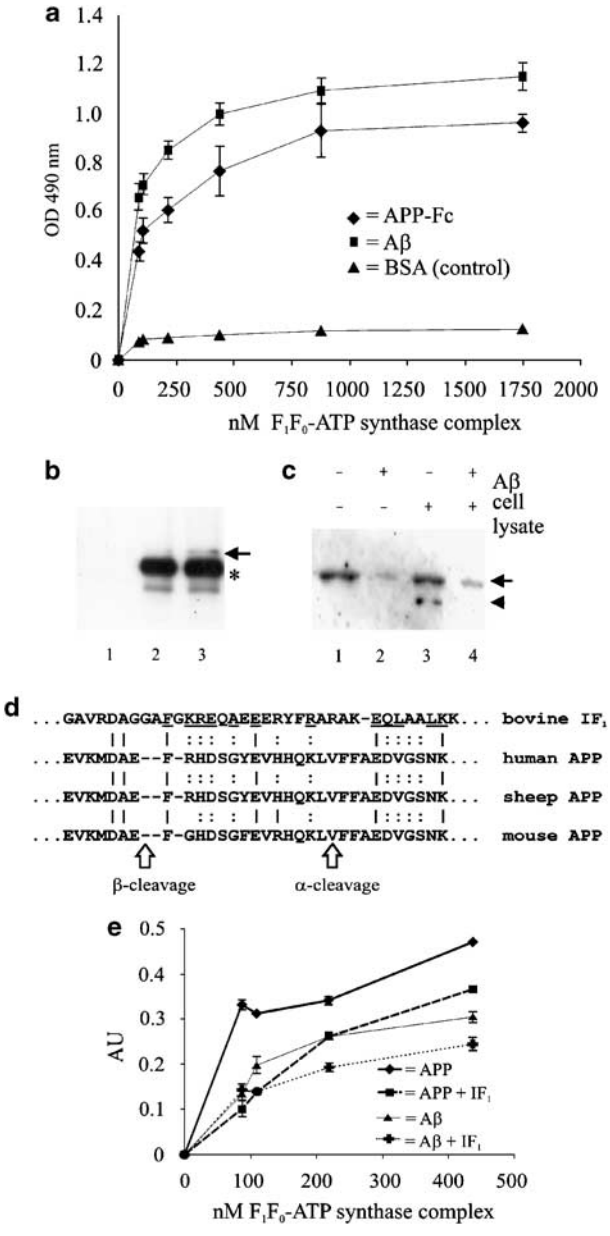

Figure 3 Purified murine ATP synthase subunit α binds to immobilized amyloid precursor protein (APP)-Fc and synthetic Aβ1–40 via the amino acid stretch 1–28 of the Aβ sequence. This stretch shows sequence similarities with the minimal inhibitory sequence of IF_1. (**a**) A total of 10 μg ml^{-1} of APP-Fc or Aβ were substrate-coated and incubated with different concentrations of soluble-purified murine ATP synthase subunit α. Binding was evaluated by ELISA using monoclonal 7H10 antibody (1:500) and secondary anti-mouse IgG HRP-coupled antibody (1:10 000) for detection. Binding of different concentrations of ATP synthase subunit α to 10 μg ml^{-1} bovine serum albumin (BSA) served as control. Mean values ± s.d. ($n = 6$). (**b** and **c**) Aβ interferes with the interaction between APP and ATP synthase subunit α. (**b**) Pull-down experiment with 50 μg APP-Fc as bait in a crude brain mitochondrial fraction supplemented with a 10-fold excess of Aβ or control peptide. Lane 1, Protein-A-coupled beads only; lane 2, Protein-A beads coupled to APP-Fc in the presence of Aβ; lane 3, Protein-A beads coupled to APP-Fc in the presence of control peptide (395–410 aa in human APP). Asterisk indicates nonspecifically pulled down bands. Arrow, ATP synthase subunit α. (**c**) Cell surface localization of ATP synthase subunit α is decreased after a 30 min pre-incubation of APP 695-transfected B103 cells with 5 μM Aβ. Lane 1, APP 695-transfected B103 cells; lane 2, APP 695-transfected B103 cells pre-incubated with 5 μM Aβ; lane 3, APP 695-transfected B103 cells pre-incubated with cell lysate containing ATP synthase subunit α; lane 4, APP 695-transfected B103 cells pre-incubated with cell lysate with Aβ. All samples were adjusted for equal protein content. Arrow, glycosylated ATP synthase subunit α; arrowhead, non-glycosylated ATP synthase subunit α. (**d**) Identification of a putative minimal inhibitory sequence of ATP synthase complex in APP. Alignment of the minimal inhibitory sequence of bovine IF_1 (residues 14–48) with the putative binding sequence of ATP synthase subunit α in APP. The α- and β-secretase cleavage sites in APP are indicated by arrows. Identical amino acids are marked by '|', conservative substitutions of amino acids between IF_1 and APP are marked by ':'. To define conservative substitutions the PAM250 scoring matrix was used. (**e**) Recombinant IF_1 competes for the binding of APP-Fc and Aβ to ATP synthase subunit α. A total of 5 μg ml^{-1} of APP-Fc and Aβ was substrate coated and incubated for 1 h with different concentrations of soluble-purified murine F_1F_0-ATP synthase complex in the presence or absence of IF_1 in a 1:1 molar ratio to Aβ and APP at pH 6.8 in incubation buffer. Binding was evaluated by ELISA using monoclonal 7H10 antibody (1:500) and secondary anti-mouse IgG HRP-coupled antibody (1:10 000) for detection. Binding of ATP synthase subunit α to 5 μg ml^{-1} BSA served as control and was subtracted. Mean values ± s.d. ($n = 4$).

influenced by pre-incubation of the APP 695-transfected B103 cells with Aβ. Also in this case, Aβ inhibited binding of ATP synthase subunit α to the cell surface of APP 695-transfected B103 cells (Figure 3c, compare lanes 3 and 4). Thus, binding of both N-glycosylated and non-glycosylated mitochondria-derived ATP synthase subunit α to cell surface-localized APP was reduced by pre-incubation with Aβ. These observations indicate that APP binds to ATP synthase subunit α via the membrane proximal domain that is represented by Aβ.

APP and Aβ both display sequence homologies with the IF_1 protein, a known natural inhibitor of the mitochondrial F_1F_0-ATP synthase complex,[43] in its minimal inhibitory domain as tested by the ScanProsite program (Figure 3d). Interestingly, this sequence similarity of APP is shared between human, sheep and mouse, and the sequence localizes in the APP domain that is cleaved by the α- and β-secretases. Indeed, recombinant human IF_1 competed for binding of APP and Aβ to the F_1 domain of ATP synthase in the ELISA test (Figure 3e).

APP and ATP synthase subunit α show partial colocalization in hippocampal cell cultures by immunocytochemistry

To analyze whether APP and Aβ are found in close association with each other in a native cellular environment, immunocytochemical staining of hippocampal neurons and astrocytes was performed by double labeling using antibodies against APP and ATP synthase subunit α (Figures 4 and 5). Live cells were used for immunolabeling to detect antigens only at the cell surface. ATP synthase subunit α appeared on neurons in a punctate manner (Figure 4) and on astrocytes in a more uniform labeling pattern (Figure 5). Secondary antibody alone or an antibody against the intracellularly localized cytoskeleton protein τ showed staining neither on neurons nor on astrocytes (data not shown). This punctate staining pattern partially overlapped with synaptophysin staining (open arrows), a marker for synapses, and was also seen in areas negative for synaptophysin (closed arrows), suggesting that cell surface ATP synthase subunit α is present in synaptic and non-synaptic areas at the neuronal plasma membrane (Figure 4B). APP and ATP synthase subunit α showed a partial colocalization at the cell surface of hippocampal neurons with 64% of ATP synthase subunit α-stained regions being also positive for cell surface APP (Figure 4Ci). This result and the finding that a the faint band of ATP synthase subunit α was detected at the cell surface by immunostaining in the APP-deficient B103 cells (Figure 2e, lane 1) suggest the presence of an additional binding partner of ATP synthase subunit α at the neuronal cell surface. The punctate staining pattern of ATP synthase subunit α on neurons is in agreement with observations on the punctate appearance of cell surface ATP synthase subunit α on hepatocytes[21] and on a human umbilical vein endothelial cell line.[33] The localization of APP and ATP synthase subunit α at the cell surface of astrocytes was less punctate, and the continuous labeling showed more overlap with the staining of APP than in neurons (Figure 5).

ATP synthase subunit α reaches the cell surface via the secretory pathway and is N-glycosylated during this process

The observation that ATP synthase subunit α is detectable at the neural cell surface raises the question of how it reaches the cell surface. We thus sought to investigate whether the enzyme is transported to the cell surface via the secretory pathway involving the Golgi apparatus. Brefeldin A was used to block transport from the endoplasmic reticulum to the Golgi apparatus. We then analyzed whether ATP synthase subunit α was detectable at the cell surface after this treatment. Cell surface biotinylation was used to specifically detect the enzyme at the cell surface and not in intracellular compartments. In the absence of brefeldin A, biotinylated ATP synthase subunit α was detectable at the cell surface (Figure 6a, lane 1). In the presence of brefeldin A, ATP synthase subunit α was not detectable as a biotinylated cell surface component (Figure 6a, lane 2).

Since proteins glycosylated in passage through the secretory pathway acquire a higher apparent molecular weight, ATP synthase subunit α was isolated after cell surface biotinylation of the neuroblastoma cell line B103. The molecular weight of the biotinylated enzyme was compared to that of ATP synthase subunit α isolated from the crude brain mitochondrial fraction. The molecular weight of the cell surface-localized ATP synthase subunit α was higher than that isolated from the mitochondrial fraction (data not shown). When the neuronal isoform of APP, the so-called APP 695 form, was transfected into APP-negative B103 neuroblastoma cells, the biotinylated cell surface form of ATP synthase subunit α was detectable and isolated using streptavidin-conjugated beads. The synthase was then digested with PNGase F, an enzyme that deglycosylates glycoproteins with *N*-linked sugars. Murine ATP synthase subunit α contains a potential N-glycosylation site at amino acid sequence position 356 (SWISS-PROT accession number Q03265) as predicted by the ScanProsite program. After PNGase F treatment, a shift in the molecular weight of ATP synthase subunit α to the molecular weight of the non-glycosylated mitochondrial ATP synthase subunit α was observed (Figure 6b, compare lane 1 with lanes 2 and 3), thus confirming N-glycosylation of the cell surface-expressed form of ATP synthase.

Soluble APP-Fc and Aβ inhibit F_1F_0-ATP synthase complex activity

Since ATP synthase subunit α is a member of the F_1 component of the mitochondrial F_1F_0-ATP synthase complex and regulates ATP production by the ATP synthase subunit β,[44] we asked whether binding of APP or Aβ to the ATP synthase subunit α would

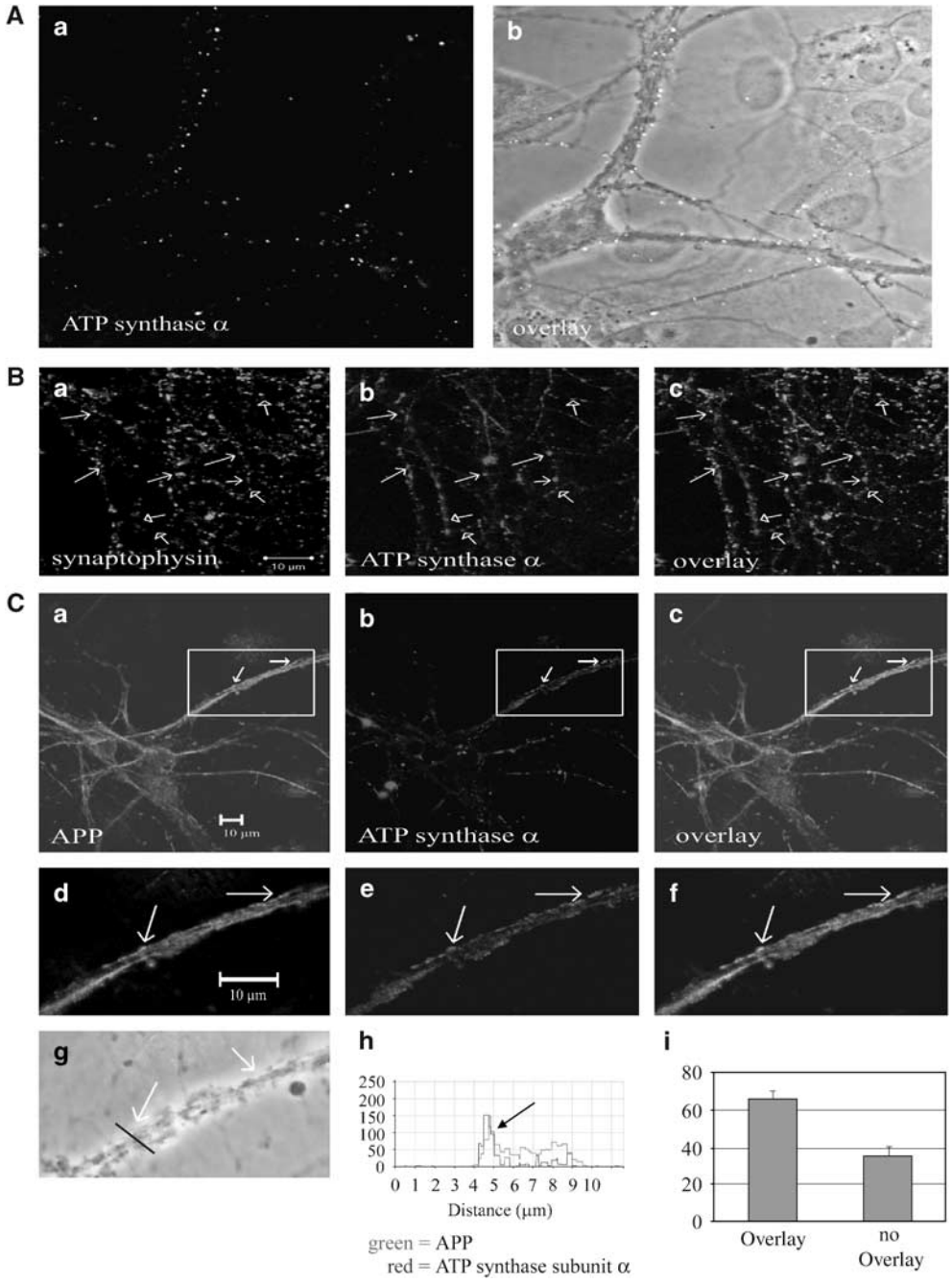

Figure 4 ATP synthase subunit α partially colocalizes with amyloid precursor protein (APP) at the cell surface in cultures of dissociated early postnatal hippocampal neurons. (**A**) (**a**) Live cell staining with ATP synthase subunit α antibody 7H10; (**b**) overlay of (**a**) and phase contrast image. (**B**) (**a**) Staining for synaptophysin in green; (**b**) live cell staining for ATP synthase subunit α in red; (**c**) overlay of (**a**) and (**b**). Open arrows indicate colocalization of ATP synthase subunit α and synaptophysin and closed arrows ATP synthase subunit α at the cell surface without synaptophysin staining. (**C**) (**a**) Live cell staining with APP antibody 22734 in green; (**b**) live cell staining with ATP synthase subunit α antibody 7H10 in red; (**c**) overlay of (**a**) and (**b**); (**d–f**) enlarged insets from (**a–c**); (**g**) enlarged inset of overlay and phase contrast image; (**h**) line intensity profile of APP (green) and ATP synthase subunit α (red) at the indicated black line in (**g**); (**i**) diagram shows percentage of overlay of ATP synthase subunit α staining at the cell surface with APP staining ± s.d. Cells were maintained in culture for 13 days. Arrow in (**h**) indicates the overlapping peak of immunofluorescence localization.

influence the function of F_1F_0-ATP synthase complex. We thus investigated whether APP or Aβ influences the oligomycin-sensitive hydrolysis of ATP in an isolated F_1F_0-ATP synthase complex fraction derived from cultures of primary human fibroblasts (Figure 7a). APP-Fc inhibited ATPase activity of the F_1F_0-ATP synthase complex by approximately 45%, whereas human Fc alone or the fusion protein of the

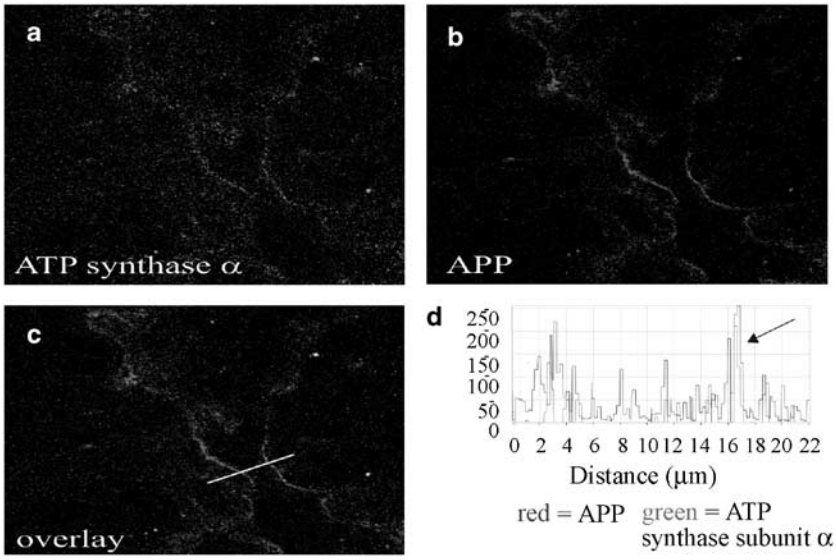

Figure 5 ATP synthase subunit α partially colocalizes with APP at the cell surface in cultures of dissociated early postnatal astrocytes; (**a**) live cell staining with antibody APP 22734 in red; (**b**) with ATP synthase subunit α 7H10 in green; (**c**) overlay of (**a**) and (**b**); (**d**) line intensity profile of amyloid precursor protein (APP, red) and ATP synthase subunit α (green) at the indicated white line in (**c**). Arrow indicates overlapping peaks of immunofluorescence localization.

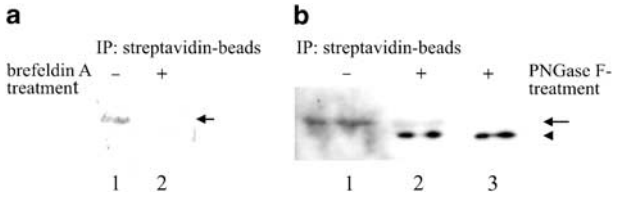

Figure 6 ATP synthase subunit α reaches the cell surface via the secretory pathway and is N-glycosylated in this process. (**a**) Effect of brefeldin A on cell surface biotinylation of ATP synthase subunit α in B103 cells transfected to express APP 695. Lane 1, cell surface biotinylation without brefeldin A treatment; lane 2, biotinylation after brefeldin A treatment. Biotinylated proteins were isolated using streptavidin beads and probed by western blot analysis using ATP synthase subunit α antibody 7H10 and APP antibody 22C11. Arrow, ATP synthase subunit α; arrowhead, APP. (**b**) Digestion of cell surface ATP synthase subunit α with PNGase F. Lane 1, cell surface biotinylation in APP 695-transfected B103 cells without PNGase F treatment; lane 2, with treatment; lane 3, crude brain mitochondrial homogenate with treatment (control). Arrow, glycosylated ATP synthase subunit α; arrowhead, non-glycosylated ATP synthase subunit α.

extracellular domain of prion protein fused to Fc (PrP-Fc) only inhibited F_1F_0-ATP synthase complex activity by approximately 10%.

A bioluminescent luciferase assay was then performed to measure ATP production at the cell surface. In this assay system, ATP generated at the cell surface and diffusing into the extracellular space of cultured cells can be determined.[19] C6 astrocytoma cells were used to measure extracellular production of ATP in the presence and absence of soluble APP-Fc and Aβ (Figure 7b). In the presence of either APP-Fc or Aβ, extracellular production of ATP was reduced by approximately 25–30% compared to the control peptide derived from a different extracellular domain of APP than Aβ. Treatment with APP-Fc did not influence intracellular levels of ATP (Figure 7c). As a control, extracellular production of ATP was monitored in the absence of ADP as substrate for the F_1F_0-ATP synthase complex that resulted in insignificant levels of ATP production. As a positive control for inhibition, piceatannol, a potent inhibitor of F_1F_0-ATP synthase complex activity, was also used and abolished the extracellular production of ATP.

To verify that C6 astrocytoma cells carry the entire ATP synthase complex at the cell surface, the F_1F_0-ATP synthase complex inhibitor IF_1 was incubated with live cells, and extracellular ATP levels were measured in a concentration-dependent manner (Figure 7d). IF_1 specifically inhibits ATPase activity of the F_1F_0-ATP synthase complex and should thus lead to an increase of ATP concentration. In the presence of IF_1, C6 astrocytoma cells showed a dose-dependent increase in ATP concentration. Given that this inhibitor is membrane impermeable and acts specifically to inhibit this complex, these observations prove that functional F_1F_0-ATP synthase complex is expressed at the cell surface of these cells.

Aβ impairs synaptic plasticity via inhibition of the F_1F_0-ATP synthase complex

To investigate the functional importance of Aβ binding to ATP synthase subunit α, we recorded LTP at the synapses formed by pyramidal cells of the CA3 subfield of the mouse hippocampus onto apical pyramidal cell dendrites of the CA1 subfield. In agreement with previous studies showing inhibitory effects of oligomeric forms of Aβ on synaptic

plasticity,[40,45] we observed a decrease in STP and LTP when TBS was applied in the presence of Aβ. The levels of STP and LTP were 200.7±13.1 and 132.2±2.6%, respectively, in nontreated control versus 134.2±8.2 and 111.9±3.3% in Aβ-treated slices (Figure 8a). If Aβ impairs LTP via inhibition of the F_1F_0-ATP synthase complex, one can expect that the inhibitor of the complex, IF_1, would mimic the effects of Aβ. Indeed, the levels of STP (146.9±8.2%) and LTP (110.5±1.5%) induced in the presence of IF_1 were not statistically different from the values found after application of Aβ (Figure 8a). Neither Aβ nor IF_1 affected basal levels of synaptic transmission before induction of LTP. Similar results were also obtained with a peptide derived from the minimal inhibitory sequence of IF_1[43] (data not shown).

Since both STP and LTP were strongly inhibited by Aβ and IF_1, we hypothesized that these compounds may elevate inhibitory transmission, thus preventing induction of both short- and long-term synaptic plasticity. To test this hypothesis, we repeated the above-described experiments in the presence of the $GABA_A$ receptor antagonist picrotoxin. The levels of STP were 246.2±28.7, 233.4±15.3 and 196.6±18.9% in slices treated with picrotoxin, picrotoxin plus Aβ and picrotoxin plus IF_1, respectively. There were no significant differences in the levels of STP between the groups. LTP levels were also not significantly different, being 151.3±8.5, 144.4±3.0 and 144.4±12.7%, respectively (Figure 8b). Thus, disinhibition of slices with picrotoxin fully abrogated the negative effects of Aβ and IF_1 on synaptic plasticity.

Theta-burst stimulation applied in the presence of picrotoxin leads to more pronounced depolarization of postsynaptic neurons that in the absence of picrotoxin. To compensate for this difference in depolarization levels and avoid saturation of LTP, we also induced LTP in the presence of picrotoxin using a weaker induction protocol, with only half the number of stimulation pulses. The levels of STP and LTP induced under these conditions in Aβ-treated (178.03±6.9 and 131.3±3.2%) and IF1-treated (186.4±7.6 and 132.7±3.1%) slices were not were not different from controls (Figures 8a and c). Thus, abrogation of Aβ and IF_1 effects on LTP by picrotoxin is not due to saturation of LTP. The fact that impairment of LTP by Aβ can be fully mimicked by IF_1 and the effects of both compounds, Aβ and IF_1,

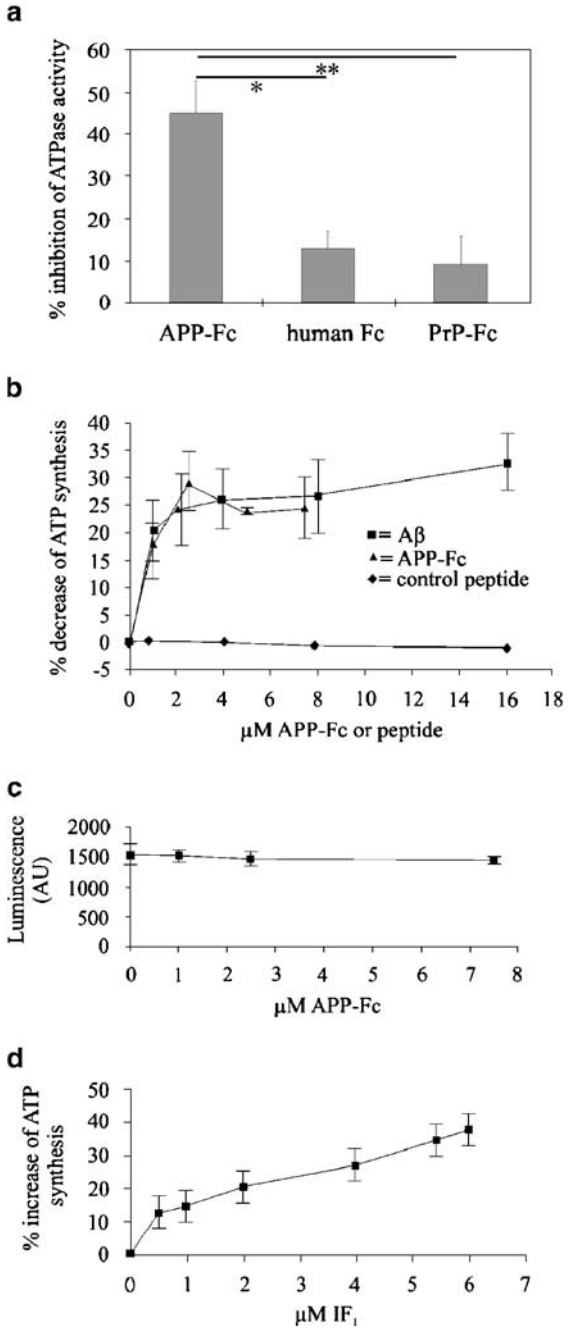

Figure 7 Amyloid precursor protein (APP) and Aβ influence ATPase and ATP synthase activity of F_1F_0-ATP synthase complex. (**a**) Inhibition of ATPase activity of mitochondrial F_1F_0-ATP synthase complex in cultured primary human fibroblasts in the presence of APP-Fc. Inhibition of ATPase activity by oligomycin, a specific inhibitor of F_1F_0-ATP synthase, was set as 100%. Mean values±s.d. ($n=5$) are shown; Kruskal–Wallis test shows $P=0.0075$ followed by Dunn's multiple comparison with $^*P<0.05$ for APP-Fc versus human Fc and $^{**}P<0.01$ for APP-Fc versus PrP-Fc. (**b**) APP and Aβ inhibit extracellular ATP production by C6 astrocytoma cells. ATP production after application of ADP was measured after 45 min incubation with APP-Fc, Aβ or control peptide by the bioluminescent luciferase assay, with total extracellular ATP production without additives being set to 100%. ATP production at the cell surface of C6 cells was inhibited in the presence of increasing concentrations of Aβ and APP-Fc. A control peptide (395–410 aa of human APP) was inactive. (**c**) Intracellular ATP production by C6 cells was not affected by 45 min incubation with APP-Fc. (**d**) Extracellular ATP production was dose dependently enhanced by IF_1, a membrane impermeable inhibitor of the ATPase activity of the F_1F_0-ATP synthase complex. Mean values±s.d. ($n=4$) are shown.

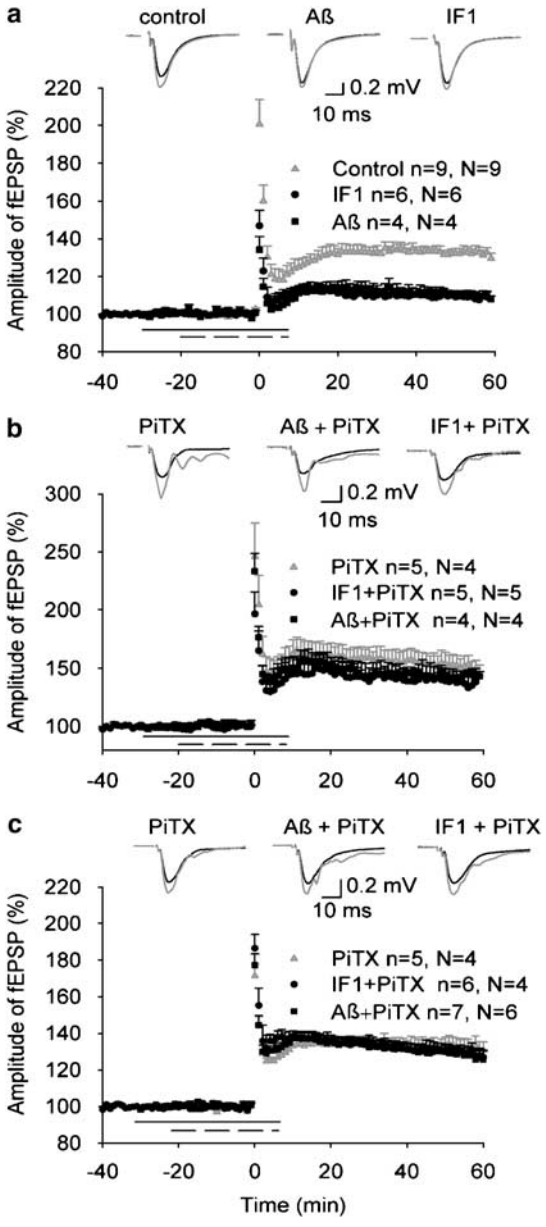

Figure 8 Aβ and the antagonist of the F_1F_0-ATP synthase complex, IF_1, have a similar mode of action on short- and long-term synaptic plasticity. (**a** and **b**) Aβ and IF_1 strongly inhibit STP and LTP induced by TBS at time '0' (**a**), whereas the antagonist of $GABA_A$ receptor picrotoxin (PiTX) co-applied with Aβ or IF_1 fully restores the levels of synaptic plasticity (**b**). (**c**) Normal levels of synaptic plasticity in Aβ- or IF_1-treated slices were elicited in the presence of picrotoxin by a protocol with a two times smaller number of stimulation pulses than used in (**a**) and (**b**). Note that the levels of LTP are similar in the control group shown in (**a**) and all groups shown in (**c**). Time intervals for application of Aβ and IF_1 are indicated by horizontal dashed and solid lines, respectively. The mean amplitude of fEPSPs evoked during 10 min preceding TBS is taken as 100%. Data show means + s.e.m.; *n* indicates the number of slices and *N* indicates the number of mice in each group. Insets show averaged fEPSPs recorded 10 min before and 50–60 min after TBS.

can be abrogated by blockade of GABAergic transmission highlights the similarity of mechanisms by which Aβ and IF_1 act on synaptic plasticity.

Discussion

In the present study we demonstrate that the extracellular domain of APP and its cleavage fragment Aβ interact with ATP synthase subunit α. The observation that Aβ competes with APP for binding to ATP synthase subunit α suggests that APP indeed binds via the stretch of 28 amino acids from the β-secretase cleavage site to the membrane-proximal portion of the molecule. The protease, α-secretase, can cleave in the middle of extracellular region of Aβ, which is also in the middle of this binding stretch. This cleavage results in an impairment of the APP–ATP synthase subunit α interaction as shown by the inability of APP-α-Fc, the APP fragment comprising the sequence from the N terminus to the α-secretase cleavage site, to pull down ATP synthase subunit α.

Transfection of APP into APP-deficient B103 neuroblastoma cells increases levels of ATP synthase subunit α at the cell surface. Increased levels of extracellular ATP synthase subunit α can be generated either by facilitating transport through the secretory pathway, or by providing a receptor for the secreted protein at the cell surface. Our data do not allow us to distinguish between these possibilities. However, we could demonstrate that transfection of B103 cells with full-length APP resulted in increased binding of supplemented soluble ATP synthase subunit α to live cultured cells, thus supporting the idea that APP serves to bind ATP synthase at the cell surface. In addition, it was not only shown that ATP subunit α is present at the cell surface but also that the subunit α is a part of a competent multi-subunit F_1F_0-ATP synthase complex.[20–22,35]

The transport of ATP synthase subunit α to the cell surface is sensitive to brefeldin A, a specific blocker of protein translocation from the endoplasmic reticulum to the Golgi apparatus. This observation indicates that cell surface–localized ATP synthase subunit α is transported via the secretory pathway to the cell surface, providing additional proof that the enzyme reaches the cell surface via a well-established processing pathway. ATP synthase subunit α at the cell surface is N-glycosylated at the arginine on position 356, the only putative N-glycosylation site. This N-glycosylation was identified by digestion of ATP synthase subunit α derived from cell surface plasma membranes with the enzyme PNGase F, which cleaves *N*-linked sugar chains.

The α subunit is an essential component of the F_1 domain of ATP synthase and regulates production of ATP by the catalytic β subunit.[41] Thus, modification of ATP synthase activity could result from binding of the extracellular domain of APP and Aβ to the α subunit. APP inhibited the oligomycin-sensitive ATPase function of this complex. We also showed that APP or Aβ binding to ATP synthase at the cell

surface inhibits extracellular ATP production. To assure that only ATP production by cell surface ATP synthase was measured, the assay was performed without addition of ADP, which is the substrate for the generation of ATP by ATP synthase. No ATP production was detected in this case.

APP and Aβ share sequence similarities with the best-described natural inhibitor of ATP synthase, namely IF_1. IF_1 is a basic protein with 84 amino acids that bind to ATP synthase subunits α, β and γ, resulting in inhibition of ATPase function of the ATP synthase complex.[36] Thus, in the presence of IF_1, ATP levels are increased. Recombinant IF_1 and a peptide with the minimal inhibitory sequence of IF_1[43] compete with Aβ and APP for binding to the purified ATP synthase complex. These experiments were conducted at pH 6.8, because the binding of IF_1 to ATP synthase is pH dependent and favored at acidic pH.[36] Similar results were obtained at pH 7.0 (unpublished observation). IF_1 inhibits the activity of ATP synthase also at physiological pH 7.3, but to a lesser extent than at acidic pH.[46] Interestingly, the RHS amino acid sequence in the putative binding domain of Aβ to ATP synthase subunit α shows a high degree of homology to the minimal inhibitory sequence of IF_1. This sequence is also reported to be responsible for binding of Aβ to α5β1 integrin.[47] Our results showing IF_1-sensitive extracellular generation of ATP by the glioma C6 cell line lead us to the conclusion that in this cell type there must also be a competent F_1F_0-ATP synthase complex at the cell surface, which could also be shown for other cell types.[20–22,35]

Another known inhibitor of ATP synthase subunit α activity is angiostatin, a proteolytically derived 38 kDa fragment of plasminogen.[19,35] This interaction has been suggested to trigger the caspase-dependent apoptotic pathway in endothelial cells[48] and cytotoxicity in non-endothelial cells.[49] Angiostatin also counteracts acetylcholine-induced vasodilation,[50] thereby decreasing cerebral blood flow. Similar activities have been reported for Aβ, which inhibits cerebral blood flow, counteracts acetylcholine activity on blood vessels, inhibits angiogenesis and is cytotoxic for endothelial cells.[51,52] The effect of Aβ on cell surface-associated ATP synthase complex in endothelial cells may account for the cerebral amyloid angiopathy aspect of Alzheimer's disease pathology.

In contrast to angiostatin, which completely inhibits extracellular ATP production, Aβ and APP inhibit only approximately one-third of the extracellular ATP production in a C6 glioma cell line. This difference in inhibitory capacity may be due to separate pools of cell surface-localized F_1F_0-ATP synthase complex that are not equally accessible to APP/Aβ and angiostatin. Also, dimerization or oligomerization of Aβ or APP may influence the interaction with the enzyme. This is conceivable, since the interaction between IF_1 and the ATP synthase complex is regulated via the oligomerization status of IF_1,[17] and it is likely that this is also the case for Aβ.

Previously, ATP synthase was shown to be present on the cell surface of hepatocytes, a 3T3 fibroblast-like cell line and umbilical vein endothelial cells.[19,35] Now, we find that ATP synthase subunit α is also present at the cell surface of murine hippocampal neurons and astrocytes as well as on the murine neuroblastoma cell line B103. Thus, neural cells express ATP synthase subunit α not only in mitochondria, but also at the cell surface. The punctate appearance of ATP synthase subunit α immunostaining at the cell surface of primary hippocampal neurons is interesting with regard to previous observations that this enzyme is found at the cell surface of hepatocytes in lipid-rich microdomains[21] and in caveolae/lipid-enriched microdomains of non-neural cells.[53] Interestingly, APP has been reported to behave as an atypical lipid raft protein.[54] It is important in this respect that both the Aβ generating β- and γ-secretases cleave APP predominantly in these microdomains,[55–56] indicating that the neurotoxic Aβ may be generated in distinct subdomains at the membrane surface, most likely in the close vicinity of ATP synthase subunit α. These microdomains appear as punctate areas on cultured hippocampal neurons. Expression of cell surface ATP synthase subunit α also overlaps partially by immunocytochemistry with the synaptic marker synaptophysin, suggesting its involvement in synaptic processes, at least in a subset of synapses. Since cell surface ATP synthase subunit α was also detected extrasynaptically and on astrocytes, it may additionally affect synaptic functions indirectly.

It is noteworthy that primary cortical neurons exposed to Aβ show a significant upregulation of ATP synthase subunit α expression.[57] This increased expression of ATP synthase subunit α could be the result of a compensatory cellular response to the inhibition of ATP synthase complex functions following APP or Aβ binding. It is thus of interest that in a mouse model of senescence, antisense oligonucleotides reacting with APP mRNA decrease the levels of ATP synthase subunit α.[58]

New models of Alzheimer's disease also include negative effects of intracellular Aβ in neurons,[59] and several findings have led to the hypothesis that an impairment of the electron transport chain in mitochondria is responsible for this pathology.[60] Recent publications and our findings describe a mitochondrial localization for APP[61] (Supplementary Figure 1), for a functional γ-secretase complex[62] and for Aβ.[63,64] Thus APP and Aβ in mitochondria could inhibit the ATP synthase subunit α within the F_1F_0-ATP synthase complex of the electron transport chain, resulting in ATP depletion. It is noteworthy in this respect that mitochondria in cultured neurons display spontaneous changes in mitochondrial membrane potential,[65] which are impaired in mitochondria from Alzheimer's disease patients.[66]

It is generally believed that one of the first signs of Alzheimer's disease pathology is a disruption of neural circuits involved in memory formation. Soluble species of Aβ reduce LTP,[67] a form of synaptic

plasticity associated with learning and memory. In our experiments Aβ reduces STP and LTP, and IF_1 mimics the effects of Aβ, suggesting that both compounds affect synaptic plasticity at CA3-CA1 synapses via inhibition of F_1F_0-ATP synthase. The possibility that IF_1 could impair LTP provides important evidence that there is a functional F_1F_0-ATP synthase complex at the cell surface of neurons and/or glial cells in the hippocampus *in situ* and that this complex could influence synaptic functions. Because IF_1 only inhibits the ATPase aspect of the ATP synthase complex, the effect must be mediated by decreasing or preventing hydrolysis of extracellular ATP. Other ectonucleotidases, so-called apyrases, can degrade extracellular ATP and thus modulate ATP-dependent signaling in the brain.[68] Therefore, the ATPase aspect of extracellularly located F_1F_0-ATP synthase complex may be important only in distinct localizations or conditions when activities of apyrases would not be sufficient to overcome an Aβ-elicited deficit in ATPase activity of F_1F_0-ATP synthase. Our experiments showing that the effects of Aβ and IF_1 on synaptic plasticity are abrogated by picrotoxin, an antagonist of GABAergic transmission, suggest that activity of the F_1F_0-ATP synthase is important for activity of GABAergic interneurons during TBS.

If Aβ inhibits degradation of extracellular ATP, synaptic plasticity could be affected in at least two ways. First, synaptic mechanisms could be directly influenced via ATP receptors expressed by neural cells, including interneurons and astrocytes. These receptors have many functions in the central and peripheral nervous systems.[69] Inhibition of ATP hydrolysis by Aβ and subsequent activation of ATP receptors could explain the observation that Aβ enhances extracellular ATP-dependent calcium waves in astrocytes.[70] However, the observed effects of Aβ via F_1F_0-ATP synthase on synaptic plasticity do not depend on the A1 adenosine receptor, because the A1 antagonist 8-cyclopentil-1,3-dipropylxanthine failed to abrogate Aβ- or IF_1-induced impairment of LTP in hippocampal slices (unpublished observations). It is also unlikely that P2 purinergic receptors are involved, since the P2X or P2Y receptor antagonists suramin, pyridoxalphoshate-6-azophenyl-2′, 4′-disulfonic acid and 8-cyclopentyl-1,3-dimethylxanthine failed to abrogate the effects of Aβ or IF_1 on synaptic plasticity (unpublished observations).

The second possibility how Aβ could reduce synaptic plasticity may involve a gradient-independent influx of protons into cells in response to hydrolysis of ATP. For instance, in bronchial epithelial cells, incubation with ATP results in a P2-class receptor-independent reduction in intracellular pH.[71] Thus, by blocking the ATPase-dependent proton influx into the cell, Aβ could influence local intracellular pH values and thus influence signal transduction, including signaling via Ca^{2+} channels.[72] The inhibition of proton influx could also result in a spatially restricted extracellular acidification, especially in confined compartments like the synaptic cleft. Data demonstrating that extracellular acidosis prevents induction of LTP in the CA1 region of the hippocampus[73] support the view that extracellular acidosis may mediate the influence of Aβ on LTP. Extracellular acidosis may lead to activation of the c-Jun N-terminal kinase,[74] which has been shown to mediate the inhibitory effects of Aβ on LTP.[75]

Also, it has been shown that exocytosed protons, resulting in acidification of the synaptic cleft, transiently suppress Ca^{2+} currents in mammalian cone photoreceptors.[76] Extracellular Aβ could lead to an inhibition of Ca^{2+} currents perhaps by inducing an extracellular acidosis in the synaptic cleft and resulting in an impairment of LTP and thus to an important aspect of learning and memory dysfunction as found in Alzheimer's disease pathology.

Acknowledgments

We thank Frank Plöger and Henrike Neuhoff for preliminary experiments, Fritz Buck for sequencing of protein bands, Matthias Staufenbiel for APP transgenic mice, Gerd Multhaup for the 22C11, WO-2 and 22734 antibodies, Sangram Sisodia for mouse APP 695 cDNA, Saskia Siegel and Galina Dityateva for help with hippocampal cultures and Wiebke Höppner and Sina Müthing for help with the ATPase assay. MS is New Jersey professor for spinal cord research.

References

1 Turner PR, O'Connor K, Tate WP, Abraham WC. Roles of amyloid precursor protein and its fragments in regulating neural activity, plasticity and memory. *Prog Neurobiol* 2003; **70**: 1–32.
2 Lazarov O, Lee M, Peterson DA, Sisodia SS. Evidence that synaptically released beta-amyloid accumulates as extracellular deposits in the hippocampus of transgenic mice. *J Neurosci* 2002; **22**: 9785–9793.
3 Mita S, Schon EA, Herbert J. Widespread expression of amyloid beta-protein precursor gene in rat brain. *Am J Pathol* 1989; **134**: 1253–1261.
4 Mattson MP, Chen SL. Neuronal and glial calcium signaling in Alzheimer's disease. *Cell Calcium* 2003; **24**: 385–397.
5 Kimberly WT, Zheng JB, Guenette SY, Selkoe DJ. The intracellular domain of the beta-amyloid precursor protein is stabilized by Fe65 and translocates to the nucleus in a notch-like manner. *J Biol Chem* 2001; **276**: 40288–40292.
6 Furukawa K, Barger SW, Blalock EM, Mattson MP. Activation of K^+ channels and suppression of neuronal activity by secreted beta-amyloid-precursor protein. *Nature* 1996; **379**: 74–78.
7 Barger SW, Mattson MP. Induction of neuroprotective κB-dependent transcription by secreted forms of the Alzheimer's beta-amyloid precursor. *Brain Res Mol Brain Res* 1996; **40**: 116–126.
8 Kamenetz F, Tomita T, Hsieh H, Seabrook G, Borchelt D, Iwatsubo T *et al.* APP processing and synaptic function. *Neuron* 2003; **37**: 925–937.
9 Caille II, Allinquant B, Dupont E, Bouillot C, Langer A, Muller U *et al.* Soluble form of amyloid precursor protein regulates proliferation of progenitors in the adult subventricular zone. *Development* 2004; **131**: 2173–2181.
10 Bayer TA, Cappai R, Masters CL, Beyreuther K, Multhaup G. It all sticks together—the APP-related family of proteins and Alzheimer's disease. *Mol Psychiatry* 1999; **4**: 524–528.
11 Wilquet V, De Strooper B. Amyloid-beta precursor protein processing in neurodegeneration. *Curr Opin Neurobiol* 2004; **14**: 582–588.

12 Lambert MP, Barlow AK, Chromy BA, Edwards C, Freed R, Loosatos M *et al.* Diffusible, nonfibrillar ligands derived from $A\beta_{1-42}$ are potent central nervous system neurotoxins. *Proc Natl Acad Sci USA* 1998; **95**: 6448–6453.
13 Kayed R, Head E, Thompson JL, Milton SC, Cotman CW, Glabe CG. Common structure of soluble amyloid oligomers implies common mechanism of pathogenesis. *Science* 2003; **300**: 486–489.
14 Mattson MP. Pathways towards and away from Alzheimer's disease. *Nature* 2004; **430**: 631–639.
15 Dodart JC, Mathis C, Bales KR, Paul SM. Does my mouse have Alzheimer's disease? *Genes Brain Behav* 2002; **1**: 142–155.
16 Revesz T, Ghiso J, Lashley T, Plant G, Rostagno A, Frangione B *et al.* Cerebral amyloid angiopathies: a pathologic, biochemical, and genetic view. *J Neuropathol Exp Neurol* 2003; **62**: 885–898.
17 Cabezon E, Montgomery MG, Leslie AGW, Walker JE. The structure of bovine F_1-ATPase in complex with its regulatory protein IF_1. *Nat Struct Biol* 2003; **10**: 744–750.
18 Vinogadov AD. Mitochondrial ATP synthase: fifteen years later. *Biochemistry (Mosc)* 1999; **64**: 1443–1456.
19 Moser TL, Kenan DJ, Ashley TA, Roy JA, Goodmann MD, Misra UK *et al.* Endothelial cell surface F1-F0 ATP synthase is active in ATP synthesis and is inhibited by angiostatin. *Proc Natl Acad Sci USA* 2001; **98**: 6656–6661.
20 Arakaki N, Nagao T, Niki R, Toyofuku A, Tanaka H, Kuramato Y *et al.* Possible role of cell surface H^+-ATP synthase in the extracellular ATP synthesis and proliferation of human umbilical vein endothelial cells. *Mol Cancer Res* 2003; **1**: 931–939.
21 Bae TJ, Kim MS, Kim JW, Choo HJ, Lee JW, Kim KB *et al.* Lipid raft proteome reveals ATP synthase complex in the cell surface. *Proteomics* 2004; **4**: 3536–3548.
22 Kim BW, Choo HJ, Lee JW, Kim JH, Ko YG. Extracellular ATP is generated by ATP synthase complex in adipocyte rafts. *Exp Mol Med* 2004; **36**: 475–485.
23 Fujii S. ATP- and adenosine-mediated signaling in the central nervous system: the role of extracellular ATP in hippocampal long-term potentiation. *J Pharmacol Sci* 2004; **94**: 103–106.
24 Delius JA, Kramer I, Schachner M, Singer W. NCAM 180 in the postnatal development of cat visual cortex: an immunohistochemical study. *J Neurosci Res* 1997; **49**: 255–267.
25 Stalder M, Phinney A, Probst A, Sommer B, Staufenbiel M, Jucker M. Association of microglia with amyloid plaques in brains of APP23 transgenic mice. *Am J Pathol* 1999; **154**: 1627–1631.
26 Chen S, Mantei N, Dong L, Schachner M. Prevention of neural cell death by neural adhesion molecules L1 and CHL1. *J Neurobiol* 1999; **38**: 428–439.
27 Xu X, Yang D, Wyss-Coray T, Yan J, Gan L, Sun Y *et al.* Wild type but not Alzheimer-mutant amyloid precursor protein confers resistance against p53-mediated apoptosis. *Proc Natl Acad Sci USA* 1999; **96**: 7547–7552.
28 Neuhoff H, Sassoe-Pognetto M, Panzanelli P, Maas C, Witke W, Kneussel M. The actin-binding protein profilin I is localized at synaptic sites in an activity-regulated manner. *Eur J Neurosci* 2005; **21**: 15–25.
29 Feng B, Tabas I. ABCA1-mediated cholesterol efflux is defective in free cholesterol-loaded macrophages. Mechanism involves enhanced ABCA1 degradation in a process requiring full NPC1 activity. *J Biol Chem* 2002; **277**: 43271–43280.
30 Zhao Y, Zhang W, Kho Y, Zhao Y. Proteomic analysis of integral plasma membrane proteins. *Anal Chem* 2004; **76**: 1817–1823.
31 Fernández-Vizarra E, Lopez-Perez MJ, Enriquez JA. Isolation of biogenetically competent mitochondria from mammalian tissues and cultured cells. *Methods* 2002; **26**: 292–297.
32 Kleene R, Classen B, Zdzieblo J, Schrader M. SH3 binding sites of ZG29p mediate an interaction with amylase and are involved in condensation-sorting in the exocrine rat pancreas. *Biochemistry* 2000; **39**: 9893–9900.
33 Shevchenko A, Wilm M, Vorm O, Mann M. Mass spectrometric sequencing of proteins silver-stained polyacrylamide gels. *Anal Chem* 1996; **68**: 850–858.
34 Kleene R, Yang H, Kutsche M, Schachner M. The neural recognition molecule L1 is a sialic acid-binding lectin for CD24, which induces promotion and inhibition of neurite outgrowth. *J Biol Chem* 2001; **276**: 21656–21663.
35 Moser TL, Stack MS, Asplin I, Enghild JJ, Hojrup P, Everitt L *et al.* Angiostatin binds ATP synthase on the surface of human endothelial cells. *Proc Natl Acad Sci USA* 1999; **96**: 2811–2816.
36 Burwick NR, Wahl ML, Fang J, Zhong Z, Moser TL, Li B *et al.* An inhibitor of the F1 subunit of ATP synthase (IF1) modulates the activity of angiostatin on the endothelial cell surface. *J Biol Chem* 2005; **280**: 1740–1745.
37 Das AM, Harris DA. Regulation of the mitochondrial ATP synthase in intact rat cardiomyocytes. *Biochem J* 1990; **266**: 355–361.
38 Eckhardt M, Bukalo O, Chazal G, Wang L, Goridis C, Schachner M *et al.* Mice deficient in the polysialytransferase ST8SiaIV/PST-1 allow discrimination of the roles of neural cell adhesion molecule protein and polysialic acid in neural development and synaptic plasticity. *J Neurosci* 2000; **20**: 5234–5244.
39 Evers MR, Salmen B, Bukalo O, Rollenhagen A, Bosl MR, Morellini F *et al.* Impairment of L-type Ca^{2+} channel-dependent forms of hippocampal synaptic plasticity in mice deficient in the extracellular matrix glycoprotein tenascin-C. *J Neurosci* 2002; **22**: 7177–7194.
40 Wang HW, Pasternak JF, Kuo H, Ristic H, Lambert MP, Chromy B *et al.* Soluble oligomers of beta amyloid (1–42) inhibit long-term potentiation but not long-term depression in rat dentate gyrus. *Brain Res* 2002; **924**: 133–140.
41 Scheuermann S, Hambsch B, Hesse L, Stumm J, Schmidt C, Beher D *et al.* Homodimerization of amyloid precursor protein and its implication in the amyloidogenic pathway of Alzheimer's disease. *J Biol Chem* 2001; **276**: 33923–33929.
42 Ida N, Hartmann T, Pantel J, Zerfass R, Forstl H, Sandbrink R *et al.* Analysis of heterogeneous A4 peptides in human cerebrospinal fluid and blood by a newly developed sensitive western blot assay. *J Biol Chem* 1996; **271**: 22908–22914.
43 Van Raaij MJ, Orriss GL, Montgomery MG, Runswick MJ, Fearnley IM, Skehel JM *et al.* The ATPase inhibitor protein from bovine heart mitochondria: the minimal inhibitory sequence. *Biochemistry* 1996; **35**: 15618–15625.
44 Bianchet MA, Hullihen J, Pedersen PL, Amzel LM. The 2.8-Å structure of rat liver F1-ATPase: configuration of a critical intermediate in ATP synthesis/hydrolysis. *Proc Natl Acad Sci USA* 1998; **95**: 11065–11070.
45 Xie CW. Calcium-regulated signaling pathways: role in amyloid beta-induced synaptic dysfunction. *Neuromol Med* 2004; **6**: 53–64.
46 Cabezon E, Butler PJ, Runswick MJ, Walker JE. Modulation of the oligomerization state of the bovine F_1-ATPase inhibitor protein, IF_1, by pH. *J Biol Chem* 2000; **275**: 25460–25464.
47 Matter ML, Zhang Z, Norstedt C, Ruoslahti E. The α5β1 integrin mediates the elimination of amyloid-β peptide and protects against apoptosis. *J Cell Biol* 1998; **141**: 1019–1030.
48 Veitonmäki N, Cao R, Wu LH, Moser TL, Li B, Pizzo SV *et al.* Endothelial cell surface ATP synthase-triggered caspase-apoptotic pathway is essential for k1-5-induced antiangiogenesis. *Cancer Res* 2004; **64**: 3679–3686.
49 Chi SL, Pizzo SV. Angiostatin is directly cytotoxic to tumor cells at low extracellular pH: a mechanism dependent on cell surface-associated ATP synthase. *Cancer Res* 2006; **66**: 875–882.
50 Koshida R, Jingsong O, Matsunaga T, Chilian WM, Oldham KT, Ackerman AW *et al.* Angiostatin: a negative regulator of endothelial-dependent vasodilation. *Circulation* 2003; **107**: 803–806.
51 Paris D, Townsend K, Quadros A, Humphrey J, Sun J, Brem S *et al.* Inhibition of angiogenesis by Aβ peptides. *Angiogenesis* 2004; **7**: 75–85.
52 Price JM, Chi X, Hellermann G, Sutton ET. Physiological levels of beta-amyloid induce cerebral vessel dysfunction and reduce endothelial nitric oxide production. *Neurol Res* 2001; **23**: 506–512.
53 Moser TL, Stack MS, Wahl ML, Pizzo SV. The mechanism of action of angiostatin: can you teach an old dog new tricks? *Thromb Haemost* 2002; **87**: 294–301.
54 Parkin ET, Turner AJ, Hooper NM. Amyloid precursor protein, although partially detergent-insoluble in mouse cerebral cortex, behaves as an atypical lipid raft protein. *Biochem J* 1999; **344**: 23–30.
55 Kaether C, Haass C. A lipid boundary separates APP and secretases and limits amyloid beta-peptide generation. *J Cell Biol* 2004; **167**: 809–812.

56 Vetrivel KS, Cheng H, Kim S-H, Chen Y, Barnes NY, Parent AT *et al.* Spatial segregation of γ-secretase and substrate in distinct membrane domains. *J Biol Chem* 2005; **280**: 25892–25900.
57 Lovell MA, Xiong S, Markesbery WR, Lynn BC. Quantitative proteomic analysis of mitochondria from primary neuron cultures treated with amyloid beta peptide. *Neurochem Res* 2005; **30**: 113–122.
58 Fai Poon H, Farr SA, Banks WA, Pierce WM, Klein JB, Morley JE *et al.* Proteomic identification of less oxidized brain proteins in aged senescence-accelerated mice following administration of antisense oligonucleotide directed at the Aβ region of amyloid precursor protein. *Mol Brain Res* 2005; **138**: 8–16.
59 Wirths O, Multhaup G, Bayer TA. A modified beta-amyloid hypothesis: intraneuronal accumulation of the beta-amyloid peptide—the first step of a fatal cascade. *J Neurochem* 2004; **91**: 513–529.
60 Reddy PH. Amyloid precursor protein-mediated free radicals and oxidative damage: implications for development and progression of Alzheimer's disease. *J Neurochem* 2006; **96**: 1–13.
61 Anandatheerthavarada HK, Biswas G, Robin M-A, Avadhani NG. Mitochondrial targeting and a novel transmembrane arrest of Alzheimer's amyloid precursor protein impairs mitochondrial function in neuronal cells. *J Cell Biol* 2003; **161**: 41–54.
62 Hansson CA, Frykman S, Farmery MR, Tjernberg LO, Nilsberth C, Pursglove SE *et al.* Nicastrin, presenilin, aph-1, and pen-2 form active γ-secretase complexes in mitochondria. *J Biol Chem* 2004; **279**: 51654–51660.
63 Khan SM, Cassarino DS, Abramov NN, Keeny PM, Borland MK, Trimmer PA *et al.* Alzheimer's disease cybrids replicate β-amyloid abnormalities through cell death pathways. *Ann Neurol* 2000; **48**: 148–155.
64 Caspersen C, Wang N, Yao J, Sosunov A, Chen X, Lustbader JW *et al.* Mitochondrial Aβ: a potential focal point for neuronal metabolic dysfunction in Alzheimer's disease. *FASEB J* 2005; **19**: 2040–2041.
65 Buckman JF, Reynolds IJ. Spontaneous change in mitochondrial membrane potential in cultured neurons. *J Neurosci* 2001; **21**: 5054–5065.
66 Thiffault C, Bennett JP. Cyclical mitochondrial $\Delta\Psi_M$ fluctuations linked to electron transport, F_0F_1 ATP-synthase and mitochondrial Na^+/Ca^{2+} exchange are reduced in Alzheimer's disease cybrids. *Mitochondrion* 2005; **5**: 109–119.
67 Walsh DM, Selkoe DJ. Deciphering the molecular basis of memory failure in Alzheimer's disease. *Neuron* 2004; **44**: 181–193.
68 Zimmermann H. Extracellular metabolism of ATP and other nucleotides. *Naunyn Schmiedebergs Arch Pharmacol* 2000; **362**: 299–309.
69 Fields RD, Stevens B. ATP: an extracellular signaling molecule between neurons and glia. *Trends Neurosci* 2000; **23**: 625–633.
70 Haughey NJ, Mattson MP. Alzheimer's amyloid b-peptide enhance ATP/gap junction-mediated calcium-wave propagation in astrocytes. *Neuromol Med* 2003; **3**: 173–180.
71 Urbach V, Hélix N, Renaudon B, Harvey BJ. Cellular mechanisms for apical ATP effects on intracellular pH in human bronchial epithelium. *J Physiol* 2002; **543**: 13–21.
72 Kiss L, Korn SJ. Modulation of N-type Ca^{2+} channels by intracellular pH in chick sensory neurons. *J Neurophysiol* 1999; **81**: 1839–1847.
73 Velisek L. Extracellular acidosis and high levels of carbon dioxide suppress synaptic transmission and prevent the induction of long-term potentiation in the CA1 region of rat hippocampal slices. *Hippocampus* 1998; **8**: 24–32.
74 Shimokawa N, Qiu CH, Seki T, Dikic I, Koibuchi N. Phosphorylation of JNK is involved in regulation of H(+)-induced c-Jun expression. *Cell Signal* 2004; **16**: 723–729.
75 Wang Q, Walsh DM, Rowan MJ, Selkoe DJ, Anwyl R. Block of long-term potentiation by naturally secreted and synthetic amyloid beta-peptide in hippocampal slices is mediated via activation of the kinases c-Jun N-terminal kinase, cyclin-dependent kinase 5, and p38 mitogen-activated protein kinase as well as metabotropic glutamate receptor type 5. *J Neurosci* 2004; **24**: 3370–3378.
76 DeVries SH. Exocytosed protons feedback to suppress the Ca^{2+} current in mammalian cone photoreceptors. *Neuron* 2001; **32**: 1107–1117.

Supplementary Information accompanies the paper on the Molecular Psychiatry website (http://www.nature.com/mp)